Polar Science xxx (xxxx) xxx–xxx

Contents lists available at ScienceDirect

Polar Science

journal homepage: www.elsevier.com/locate/polar

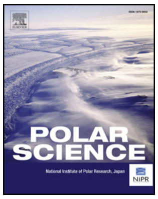

Interannual variation in solar heating in the Chukchi Sea, Arctic Ocean

Yushiro Tsukada[a], Hiromichi Ueno[a,*], Naoki Ohta[b], Motoyo Itoh[c], Eiji Watanabe[c], Takashi Kikuchi[c], Shigeto Nishino[c], Kohei Mizobata[d]

[a] *Graduate School of Fisheries Sciences, Hokkaido University, 3-1-1 Minato-cho, Hakodate, 041-8611, Japan*
[b] *Graduate School of Environmental Science, Hokkaido University, N10 W5 Kita-ku, Sapporo, 060-0810, Japan*
[c] *Institute of Arctic Climate and Environment Research, Japan Agency for Marine-Earth Science and Technology, 2-15 Natsushima-cho, Yokosuka, 237-0061, Japan*
[d] *Department of Ocean Sciences, Tokyo University of Marine Science and Technology, 4-5-7 Konan, Minato-ku, Tokyo, 108-8477, Japan*

ARTICLE INFO

Keywords:
Solar heating
Chukchi sea
Interannual variation

ABSTRACT

Solar heating in summer in the Chukchi Sea was estimated using satellite-derived sea-ice concentration data and reanalysis shortwave radiation data. The shortwave radiation was validated by *in-situ* data obtained by the R/V Mirai and NCEP-CFSR/CFSv2 was found to reproduce *in-situ* data accurately compared with NCEP/NCAR Reanalysis 1 and ERA-Interim. Solar heating integrated over the Chukchi Sea in summer varied interannually from 3.6×10^{20} J in 2000 to 6.7×10^{20} J in 2015, and was up to twice the northward heat flux through the Bering Strait. The total heating in the Chukchi Sea implies that the heat in the Chukchi Sea provided by northward heat flux through the Bering Strait is amplified by solar heating in the Chukchi Sea. We further compared these heat fluxes into the Chukchi Sea with the summertime northward heat flux through Barrow Canyon, an indicator of heat flux from the Chukchi Sea to the Arctic basin. The northward heat flux through Barrow Canyon was affected by the interannual variation of solar heating in the eastern Chukchi Sea. These results imply that modification of Pacific water in the Chukchi Sea by solar heating plays an important role in the interannual variation in heat transport from the Chukchi Sea to the western Arctic basin.

1. Introduction

Summer Arctic sea-ice cover has declined rapidly over the past few decades. The albedo of sea ice is much higher than that of open water; a decrease in sea-ice cover is associated with an increase in solar heating and thus surface warming of the Arctic Ocean (Perovich et al., 2007; Steele et al., 2008). The reduction in sea-ice cover also plays a significant role in the polar amplification of climate change (Holland and Bitz, 2003; Serreze et al., 2009) and in marine and terrestrial ecological dynamics in the Arctic region (Post et al., 2013).

The largest decline in sea ice occurred in the Pacific region of the Arctic Ocean (Comiso, 2012). Heat transport of Pacific water through the Bering Strait, which has increased in recent years (Woodgate et al., 2006, 2010; 2015), plays an important role in decreasing sea-ice formation during the winter and in sea-ice melt in summer in the Canada basin (Steele et al., 2004; Shimada et al., 2006). In 2007, which was marked by an extreme retreat of Arctic sea ice, the heat transport was sufficient to cause one third of the seasonal Arctic sea-ice loss (Woodgate et al., 2010).

The Chukchi Sea (Fig. 1) is located between the Bering Sea and the Arctic basin and is a pathway for Pacific water from the Bering Strait. We anticipate that solar heating significantly modifies Pacific water in the Chukchi Sea. However, there have been no quantitative analyses of solar heating in the Chukchi Sea except for a rough estimate of $4 \times 10^{20}\,\mathrm{J\,yr^{-1}}$ (Woodgate et al., 2010) based on an annual solar heating of $\sim 1300\,\mathrm{MJ\,m^{-2}\,yr^{-1}}$ (Perovich et al., 2007) and a Chukchi Sea area of $\sim 350 \times 10^3\,\mathrm{km}^2$. It was also indicated that the annual northward heat flux through the Bering Strait was somewhat greater than annual solar heating in the Chukchi Sea and the former interannual variation was slightly larger than the latter (Woodgate et al., 2010). In this study, we estimated interannual variation in solar heating in summer in the Chukchi Sea by analyzing satellite-derived sea-ice concentration data and reanalysis shortwave radiation data, and compared its impact on the heat budget of the Chukchi Sea with that of heat transport through the Bering Strait after validating the reanalysis data using *in-situ* shortwave radiation data obtained by the R/V Mirai.

2. Data and methods

The study area was the Chukchi Sea, comprising the shelf area between the Bering Strait and the western Arctic basin (65.45°–75°N, 155°–180°W, excluding the area where water depth was > 200 m, i.e.,

---

[*] Corresponding author. Faculty of Fisheries Sciences, Hokkaido University, 3-1-1 Minato-cho, Hakodate, 041-8611, Japan.
E-mail address: ueno@fish.hokudai.ac.jp (H. Ueno).

https://doi.org/10.1016/j.polar.2018.06.003
Received 26 December 2017; Received in revised form 9 June 2018; Accepted 11 June 2018

Please cite this article as: Tsukada, Y., Polar Science (2018), https://doi.org/10.1016/j.polar.2018.06.003

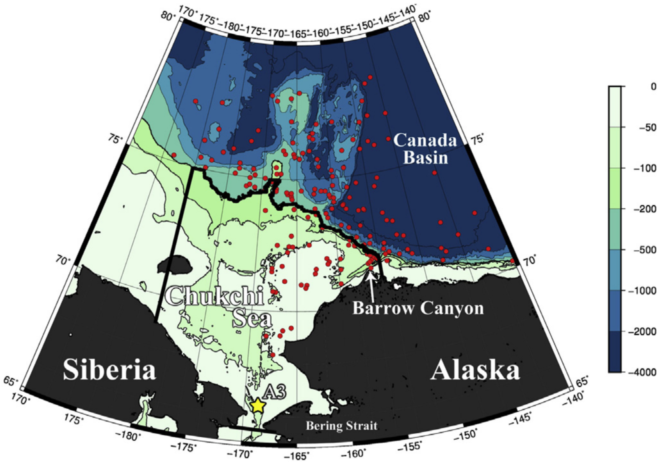

Fig. 1. Bottom topography (m) of the Chukchi Sea. The area enclosed by the solid black line indicates the area analyzed in this study (65.45°–75°N, 155°–180°W excluding the area where water depth > 200 m). Red dots indicate the locations of *in-situ* downward shortwave radiation observations by R/V Mirai (in 1999, 2002, 2004, 2006, 2008, 2009, and 2010) averaged over 24 h.

the area enclosed by the solid black line in Fig. 1). The analysis period was 1999–2015, based on the data available on heat flux through the Bering Strait (Woodgate et al., 2015) and *in-situ* shortwave radiation, as described below. The solar heating (flux of solar heat input to the ocean, F_{rw}) was calculated as follows:

$$F_{rw} = F_r\ (1\text{-}\alpha)\ (1\text{-C})\ [\mathrm{W\ m^{-2}}] \qquad (1)$$

According to Perovich et al. (2007). In eq. (1), F_r is downward shortwave radiation, α is the ocean albedo, and C is the sea-ice concentration. We used a value of 0.07 (Pegau and Paulson, 2001) for ocean albedo (α). We considered only the downward solar energy incident on the open ocean, and neglected the downward solar energy incident on/passing through the sea ice, as in Perovich et al. (2007). Recently, it is indicated that light transmission through sea-ice is important for the near-surface temperature maximum structure in Canada Basin (Jackson et al., 2010) and massive phytoplankton blooms under sea-ice in the northern Chukchi Sea (Arrigo et al., 2012). In the Chukchi Sea, it was reported that annual total solar heating through sea-ice ranges from 0.1×10^8 $\mathrm{Jm^{-2}}$ near the Bering Strait to 1×10^8 $\mathrm{Jm^{-2}}$ in the northern Chukchi Sea (Arndt and Nicolaus, 2014). Since sea-ice concentration in the Chukchi Sea is low in summer especially in the southern part, solar heating through sea-ice was much smaller than cumulative solar heating into open ocean from May to September ($3\text{–}17 \times 10^8$ $\mathrm{Jm^{-2}}$, see Fig. 5). Therefore, we neglected light transmission through sea-ice in the present study.

For sea-ice concentration (C), we used daily mean 25 km × 25 km data generated from satellite passive microwave observations using the NOAA/NSIDC Climate Data Record (Peng et al., 2013, https://climatedataguide.ucar.edu/climate-data/sea-ice-concentration-noaansidc-climate-data-record). For downward shortwave radiation (F_r), we used data from the following reanalysis products: (1) NCEP/NCAR Reanalysis 1 (Kalnay et al., 1996, http://www.esrl.noaa.gov/psd/data/gridded/data.ncep.reanalysis.tropopause.html, approximately 2° × 2°, daily), (2) ERA-Interim (Dee et al., 2011, http://www.ecmwf.int, 0.125° × 0.125°, 12-hourly) and (3) NCEP-CFSR/CFSv2 (NCEP-CFSR; hereafter, Saha et al., 2010, http://rda.ucar.edu/pub/cfsr.html, about 0.3° × 0.3° for CFSR (1999–2010), approximately 0.2° × 0.2° for CFSv2 (2011–2015), 6-hourly). We evaluated daily solar heating in the grids of the reanalysis products by linearly interpolating sea-ice concentration data to the grid of the reanalysis product. In the present study, we combined satellite sea-ice concentration data with reanalysis downward shortwave radiation data to estimate solar heating; we did not use net surface shortwave radiation data from reanalysis products. This is because (1) satellite sea-ice concentration data were more accurate than those from reanalysis products and (2) we intended to directly validate reanalysis downward shortwave radiation data with *in-situ* data as described below.

Downward shortwave radiation data differ according to the reanalysis product, particularly at high latitudes, due to the scarcity of *in-situ* observations. In this study, we used *in-situ* downward shortwave radiation data obtained by the R/V Mirai (R/V Mirai cruises MR99 [September 1999], MR02 [August–October 2002], MR04 [September–October 2004], MR06 [August–September 2006], MR08 [August–October 2008], MR09 [September–October 2009], and MR10 [September–October 2010]; http://www.godac.jamstec.go.jp/darwin/e) to validate reanalysis shortwave radiation data in the Chukchi Sea, selecting the most suitable reanalysis data set for our study. We first calculated the 24-h averaged *in-situ* downward shortwave radiation and ship positions (red dots in Fig. 1) from original Mirai data obtained every 10 min. Then, the downward shortwave radiation from the reanalysis products was also 24-h averaged, and linearly interpolated to the positions of the R/V Mirai data. Finally, the two values for the same day and location were compared (176 pairs in total). The *in-situ* data from the R/V Mirai north of the Chukchi Sea were also used because of the scarcity of *in-situ* data within the Chukchi Sea itself.

We used data from the A3 mooring (66.33°N, 168.96°W, 56 m depth) ~60 km north of the Bering Strait (Woodgate et al., 2015, http://psc.apl.washington.edu/HLD/Bstrait/Data/BeringStraitMooringDataArchive.html) during 1999–2015 to evaluate daily ocean heat transport through the Bering Strait, following Woodgate et al. (2012). The daily heat fluxes through Barrow Canyon during 1999–2014 (Itoh et al., 2013) were also used for comparison with the solar heating. For the latent heat, sensible heat and longwave radiation fluxes, we used the reanalysis data used to estimate solar heating (NCEP-CFSR, see next section). The sea-ice melting heat was calculated from the difference in the daily mean sea-ice concentration averaged over the Chukchi Sea between a given day and the previous day, assuming that the sea-ice thickness was 1 m and neglecting sea-ice advection. The value of 1 m is consistent with the average sea-ice thickness of 1.38 m previously observed in the coastal northeastern Chukchi Sea (Fukamachi et al., 2017) and a value of ~1.5 m that we derived for the Chukchi Sea during March–April using CryoSat-2 data (http://www.cpom.ucl.ac.uk/csopr/seaice.html). Our analysis was limited to the summer season (May–September), neglecting the heat release due to sea-ice formation, because sea-ice concentration generally decreases from May to August and starts to increase again in October, and heat transport through the Bering Strait is almost zero before May (Fig. 2). In the present paper, integrated values in summer season for the solar heating, heat fluxes and heat transports (with the unit of J) are discussed.

3. Validation of downward shortwave radiation from reanalysis products

The downward shortwave radiation from the reanalysis products was compared with *in-situ* data obtained by the R/V Mirai. Fig. 3 shows day-to-day variation of downward shortwave radiation from reanalysis products and *in-situ* observations. This figure indicates that the values from the reanalysis products mostly follows day-to-day variation of *in-situ* data. The values from the reanalysis products also reproduce decreasing trend of *in-situ* data during each observation period. However, the averaged downward shortwave radiation using all values in Fig. 3 was 41.0, 41.3, 71.8 and 19.8 $\mathrm{W\,m^{-2}}$ for *in-situ* observations, NCEP-CFSR, ERA Interim and NCEP-NCAR Reanalysis 1, respectively: the averaged values from ERA Interim and NCEP-NCAR Reanalysis 1 were smaller and larger than that from *in-situ* data, respectively.

The values from the reanalysis products were all significantly correlated with the *in-situ* values (at the 99% confidence level, Table 1 and